Scientific Research Publishing

Smart Grid and Renewable Energy, 2019, 10, 257-278
https://www.scirp.org/journal/sgre
ISSN Online: 2151-4844
ISSN Print: 2151-481X

Vertical Profile of Wind Speed in the Atmospheric Boundary Layer and Assessment of Wind Resource on the Bobo Dioulasso Site in Burkina Faso

Drissa Boro[1], Hagninou Elagnon Venance Donnou[2], Imbga Kossi[1], Nebon Bado[1], Florent P. Kieno[1], Joseph Bathiebo[1]

[1]Laboratoire d'Energies Thermiques Renouvelables (L.E.T.RE), Université Joseph KI-ZERBO, Ouagadougou, Burkina Faso
[2]Laboratoire de Physique du Rayonnement (LPR), Faculté des Sciences et Techniques (FAST), Université d'Abomey-Calavi, Cotonou, Benin
Email: drissaboro5@gmail

How to cite this paper: Boro, D., Donnou, H.E.V., Kossi, I., Bado, N., Kieno, F.P. and Bathiebo, J. (2019) Vertical Profile of Wind Speed in the Atmospheric Boundary Layer and Assessment of Wind Resource on the Bobo Dioulasso Site in Burkina Faso. *Smart Grid and Renewable Energy*, **10**, 257-278.
https://doi.org/10.4236/sgre.2019.1011016

Received: November 5, 2019
Accepted: November 26, 2019
Published: November 29, 2019

Abstract

This study investigates both the characteristics of the vertical wind profile at the Bobo Dioulasso site located in the Sudanian climate zone in Burkina Faso during a day and night convective wind cycle and the estimation and variability of the wind resource. Wind data at 10 m above ground level and satellite data at 50 m altitude in the atmospheric boundary layer were used for the period going from January 2006 to December 2016. Based on Monin-Obukhov theory, the logarithmic law and the power law made it possible to characterize the wind profile. On the study site, the atmosphere is generally unstable from 10:00 to 18:00 and stable during the other periods of the day. Wind extrapolation models were tested on our study site. Fitting equations proposed are always in agreement with the data, contrary to other models assessed. Based on these equations, the profile of a day and night cycle wind cycle was established by extrapolation of wind data measured at 10 m above the ground. Lastly, the model of the power law based on the stability was used to generate data on wind speed from 20 m to 50 m based on data from 10 m above the ground. Weibull function was used to characterize wind speed rate distribution and to calculate wind energy potential. The average annual power density on the site is estimated at 53.13 W/m^2 at 20 m and at 84.05 W/m^2 at 50 m, or 36.78% increase. Considering these results, the Bobo-Dioulasso site could be appropriate to build small and medium-size turbines to supply the rural communities of the Bobo Dioulasso region with electricity.

Keywords

Wind Potential, Weibull Distribution, Power Density, Vertical Profil Vertical

1. Introduction

Energy is a key factor that contributes to populations' socio-economic well-being. With the growing population coupled with development needs in terms of energy demand [1], the access to sustainable energy remains a major challenge. With the gradual depletion of traditional energy resources and their environmental impact, it is detrimental to align the energy sector development strategies with envronmental protection for sustainable development [2]. In this context, the contribution of renewable energy to the global energy mix has steadily increased [3]. Among the sources of renewable energy, wind power appears to be the most visible over these recent years because of its safety for the environment and its inexhaustible nature [4].

However, a study commissioned by the African Development Bank explicitly reveals that in the Sub-Saharan Africa and particularly in Burkina Faso, several major obstacles challenge the use and the development of this source of energy [5]. One of these obstacles is the lack of dada on wind potential within the hub to estimate the resource available. More often, the wind resource available within the hub of a wind turbine (more than 10 m) is generally assessed through the installation of large towers or even more expensive equipment, including the LIDAR system (Light Detection And Ranging) or SODAR (Sonic Detection and Ranging) to perform the measurements. These tools used to assess the resource therefore increase the cost of wind projects by making them often economically unsustainable [6].

To address this difficulty, research has been directed towards the extrapolation of wind speeds measured by observing stations already available, from a standard measurement site (10 m altitude) to another site with energy interest (level of wind turbine hub) based on empirical models applicable only in the surface layer [7] [8]. This is the case of the empirical formulas of the power law and the logarithmic law developed by several authors including [9]-[15]. However, after having tested their reliability on other sites, the authors of [4] [16] have obtained less satisfactory results. The authors therefore propose the establishment of a specific model for each site. In our study area, wind data in the hub of a wind turbine are not available, except the average NASA satellite data [17] calculated over a day at 50 m altitude. In addition, previous studies conducted on the assessment of wind resource at the study site by authors of [18] were limited to 10 m of altitude where data are measured every three hours.

Thus to solve this problem of lack of wind data on the study site at an altitude higher than 10 m, the NASA satellite data at 50 m and the data of the National Agency of Meteorology of Burkina (ANAM) at 10 m altitude were used. The best

equations for estimating the wind speed at altitude from the power law and the logarithmic law are then established. Wind shear parameters contained in these models based on the atmospheric stability conditions were then determined and a comparative study between the models available in the literature and the data was made. The most suitable model for the site was used to extrapolate the vertical day and night wind profile based on data collected at 10 m above the ground. Based on the profile obtained, we assessed the wind potential in Bobo-Dioulasso between 20 m and 50 m above the ground and studied its variability during the year.

2. Presentation of the Study Environment and Data Used

Burkina Faso, is a vast country of 274,200 square kilometers, located at the heart of West Africa, between parallels 9˚20' and 15˚05' of the North Latitude and meridians 2˚20' of the East Longitude and 5˚30' of the West longitude at an average altitude of 300 m above the sea level. It is a landlocked country surrounded by six (06) countries: Mali in the West and the North, Niger in the East, and by Benin, Togo, Ghana and Côte d'Ivoire in the South. According to the rainfall and temperatures recorded in Burkina Faso, there are 3 large climat zones. The Sahelian climat zone located in the North of the 14th parallel characterized by an annual rainfall of less than 650 mm. The Sudano-Sahelian climat zone located between the parallels 11˚30 and 14˚ of North latitude characterized by an annual rainfall ranging between 650 and 1000 mm. The Sudanese climate zone in the South with 11˚30' of North latitude, characterized by an annual rainfall above 1000 mm [19]. Our study was conducted on the Bobo-Dioulasso site (Sudanian climat zone); data recorded and provided by the meteorological station of the Burkina Faso National Meteorological Agency (ANAM) during the period from January 2006 to December 2016 were used. The series of data used included those on wind speeds and temperature. The observation was made each every three hours using a cup anemometer placed on a 10 m pole above the ground. Ambient temperature was also measured on the site, at each every three hours. Daily wind speed data recorded at 50 m above the ground and provided by the NASA Prediction of Worldwide Energy Resource (POWER) [17] during the same measurement period were used. **Figure 1** gives an overview of the study area and **Table 1** gives the geographic coordinates of the site for the study.

3. Method

3.1. Vertical Extrapolation Method of the Wind Speed

Both most widely used wind speed extrapolation methods that take into account roughness and atmospheric stability conditions [20] [21] were used, *i.e.* the log-linear law based on the similarity model and the power law [12] [13] [15] that were evaluated on our study site in order to choose the most optimal one.

3.1.1. The Log-Linear Law

This law takes into account the shear speed, the roughness length and the

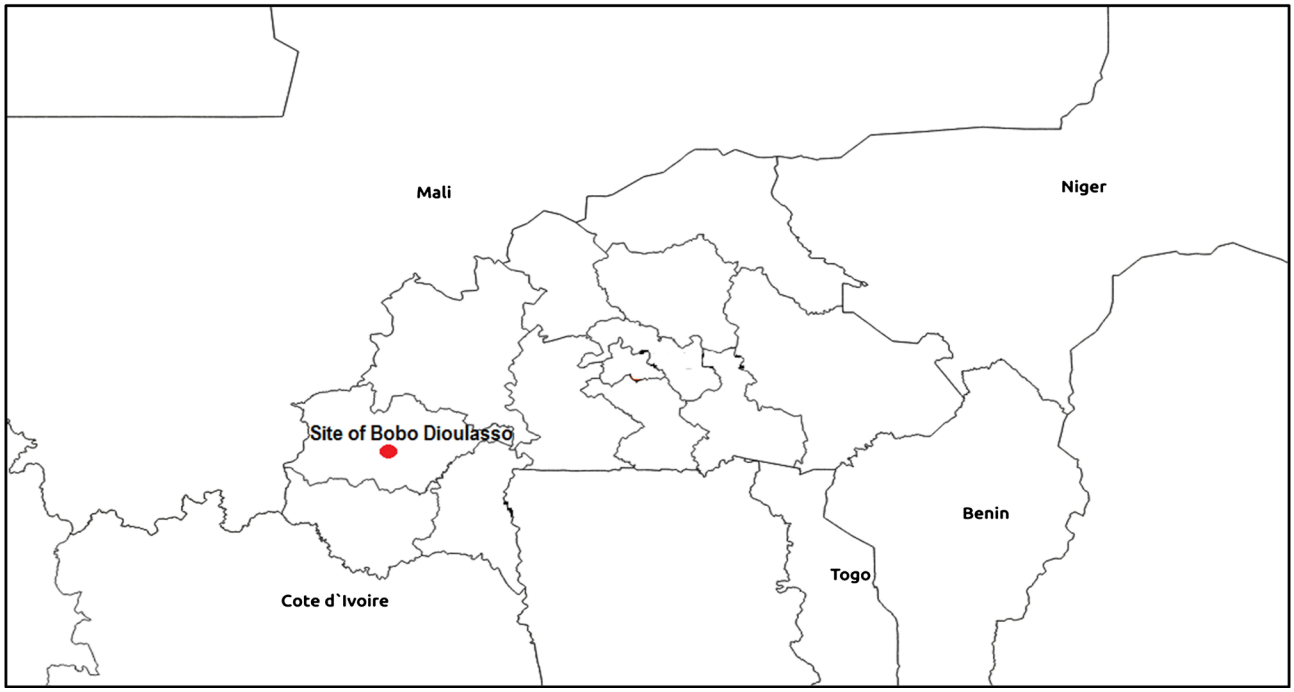

Figure 1. Geographic location of the study site.

Table 1. Geographic coordinates of the sites studies.

Site	Longitude	Latitude	Altitude (m)
Bobo Dioulasso	04˚18'W	11˚10'N	423

Monin-obukhov length. It is expressed by the following formula [9]:

$$v(z)=\left(\frac{u_*}{\kappa}\right)\left[\ln\left(\frac{z}{z_0}\right)-\psi\left(\frac{Z}{L}\right)\right] \tag{1}$$

where L, is the Monin-Obukhov length, z_0 the roughness length, u_* the friction speed in m/s, $\psi(Z/L)$ is the stability correction function, and κ the Von Karman constant assumed to be 0.4 and Z the height. The expression of the stability correction function is given by Paulson [22]. We have the following equation for unstable atmospheric conditions $(Z/L<0)$:

$$\psi_m(Z/L)=2\ln\left(\frac{1+x}{2}\right)+\ln\left(\frac{1+x^2}{2}\right)-2\arctan(x)+\frac{\pi}{2} \tag{2}$$

$$x=\left[1-\left(\frac{\gamma z}{L}\right)\right]^{1/4} \tag{3}$$

In stable atmospheric conditions $(Z/L>0)$ [22], the expression is given by the Equation (4).

$$\psi_m(Z/L)=-5(Z/L) \tag{4}$$

The method used to calculate the Monin-Obukhov length that characterizes the stability of the surface layer is based on the expression from the Monin and

Obukhov studies [9] and is given by the Equation (5):

$$L = -\frac{u_*^3 T_0}{\kappa g \operatorname{cov}(w,T)} \tag{5}$$

where $\operatorname{cov}(w,T)$ represents the covariance of the vertical wind component and the ambient air temperature, g the gravity, T_0, the average temperature, κ Von Karman constant. Based on Cauchy-Schwarz inequality which is based on covariance mathematical properties, we therefore calculated $\operatorname{cov}(w,T)$. So we have [23]:

$$\left[\operatorname{cov}(\omega,T)\right]^2 \le \sigma^2(\omega)\sigma^2(T) \tag{6}$$

where $\sigma^2(T)$ is the variance of the air temperature and $\sigma^2(\omega)$, the variance of the vertical wind component. According to [23], the standard deviation of the vertical wind component $\sigma(\omega)$ can be estimated from the parameter $\sigma(v)$ which is the standard deviation of the horizontal wind component:

$$\sigma(\omega) = 0.45\sigma(v) \tag{7}$$

where v is the horizontal wind speed recorded by the anemometer at 10 m above the ground. The results obtained with the Equation (5) during the day cycle were used to characterize the stable or unstable atmospheric conditions. **Table 2** details the various atmospheric stability classes according to Obukhov length.

The roughness length and the friction speed can be calculated according to the various stability classes of the atmosphere by changing variables and using the Equation (1) [23]:

$$u^* = \kappa P \tag{8}$$

$$z_0 = \exp\left[-\left(\frac{H}{P} + \psi\left(\frac{z}{L}\right)\right)\right] \tag{9}$$

The equation (1) therefore becomes:

$$V_h = P\ln(z_h) + H \tag{10}$$

3.1.2. Power Law

Power law was proposed by G. Hellman and is based on experimentation. This method is easier to use in general for engineering studies [24] and thus enables to address difficulties encountered in using the linear-log law in terms of input

Table 2. Atmospheric stability class according to Obukhov length [23].

Stability class	Monin-Obukov's length (m)
Very stable	$0 < L < 200$
Stable	$0 < L < 1000$
Neutral	$\lvert L\rvert > 1000$
Instable	$-200 < L < 0$
Very instable	$-1000 < L < -200$

parameters. Therefore, we have [25] [26] [27]:

$$\frac{v_h}{v_1} = v_1\left(\frac{z_h}{z_1}\right)^{\alpha} \tag{11}$$

where v_1 is the wind speed at 10 m. α is the shear coefficient of the wind. It depends on atmospheric stability and roughness [12] and provides information on the variations of wind intensity according to the altitude. Based on the Equation (11), α can be calculated by the properties of logarithms [28]:

$$\alpha = \frac{\ln(v_2) - \ln(v_1)}{\ln(z_2) - \ln(z_1)} \tag{12}$$

According to studies by Huang (1979) [29] reported by [27], the wind shear coefficient varies with unstable and stable atmospheric conditions. It is expressed by the equations (13) and (14), respectively.

$$\alpha = \frac{\left(1-16(Z/L)\right)^{-1/4}}{\ln\left((\eta-1)(\eta_0+1)/(\eta+1)(\eta_0-1)\right)+2\arctan(\eta_0)} \tag{13}$$

$$\eta = \left(1-16(Z/L)\right)^{1/4} \quad \text{et} \quad \eta = \left(1-16(Z_0/L)\right)^{1/4}$$

$$\alpha = \frac{1+5(Z/L)}{\ln(Z/Z_0)+5(Z/L)} \tag{14}$$

Based on the power law and logarithmic law, parameters α, P and H are calculated by monthly and annual data fitting. Based on the values taken by these parameters, we therefore deduce the best wind speeds extrapolation equations in altitude, using statistical error estimation tests.

3.1.3. Model Validation Test

Statistical tests of the root mean squared error (RMSE) and mean absolute value (MAE) were used to assess the errors made by the prediction. These indicators are the most used and the model is better when they are close to zero [23]. Using Equations (15) and (16), errors between speeds measured and those estimated are assessed [23] [30] [31]:

$$\text{RMSE} = \left(\frac{1}{N}\sum_{i=1}^{N}(p_i - f_i)\right)^{1/2} \tag{15}$$

$$\text{MAE} = \frac{1}{N}\sum_{i=1}^{N}\left|(p_i - f_i)\right| \tag{16}$$

where p_i represents observations, f_i the various estimates or forecasts, and N the total number of observations of wind speed.

3.2. Wind Resource Assessment Method

3.2.1. Analysis of Statistic Distribution of Wind Speed Data

Over these recent years, several distribution functions are developed and tested by several researchers around the world to identify those best suited for wind energy applications. These include beta, Erlang, exponential, gamma, log-logistic,

normal log, Pearson V, Pearson VI, uniform, and Weibull distribution functions [32] [33] [34]. On our study site, it has been demonstrated that the Weibull distribution with two parameters (shape parameter and scale parameter) developed in 1951 by Waloddi Weibull is suitable to analyze and represent the wind rate distribution. This distribution was therefore used and expressed as follows [35] [36].

$$f(v)=\left(\frac{k}{c}\right)\left(\frac{v}{c}\right)^{k-1}\exp\left[-\left(\frac{v}{c}\right)^{k}\right] \tag{17}$$

$$k>0,\quad v>0,\quad c>0$$

where k is the dimensionless Weibull shape parameter, c the scale parameter in $\mathrm{m\cdot s^{-1}}$, v the wind speed in $\mathrm{m\cdot s^{-1}}$ and $f(v)$ the probability of observing the wind speed v, or also called the frequency of occurrence. The corresponding Weibull cumulative density function $F(v)$ is given in [37]:

$$F(v)=1-\exp\left[-(v/k)^{k}\right] \tag{18}$$

The expressions of the mean wind speed v, and the standard deviation σ according to Weibull parameters are presented by the Equations (19) and (20), respectively:

$$\overline{v}=c\Gamma\left(1+1/k\right) \tag{19}$$

$$\sigma^{2}=c^{2}\left[\Gamma\left(1+2/k\right)-\Gamma^{2}\left(1+1/k\right)\right] \tag{20}$$

Γ is the gamma function expressed by the Equation (21):

$$\Gamma(x)=\int_{0}^{\infty}\exp(-t)\cdot t^{x-1}\mathrm{d}t \tag{21}$$

Several methods are used to determine Weibull parameters [38] [39] [40]. The one used in this study to calculate the Weibull parameters is the maximum likelihood method [41] [42]. The parameters of form k and scale c are estimated using the Equations (22) and (23), respectively:

$$k=\left(\frac{\sum_{i=1}^{n}V_{i}^{k}\ln V_{i}}{\sum_{i=1}^{n}V_{i}^{k}}-\frac{1}{n}\sum_{i=1}^{n}\ln V_{i}\right)^{-1} \tag{22}$$

$$c=\left(\frac{1}{n}\sum_{i=1}^{n}V_{i}^{k}\right)^{1/k} \tag{23}$$

where v_i is the wind speed at the course of time i and n is the non-zero wind speed observation number. Equation (22) can be solved using an iterative procedure ($k = 2$ is the appropriate initial conjecture), then Equation (23) is solved explicitly. Equation (22) must be used for non-zero wind speed data points only.

3.2.2. Wind Power Density

Wind energy power density is the most important feature of wind. It represents

the amount of mechanical energy produced by wind. Assuming that S is the cross-cutting section through which wind blows perpendicularly, the mean wind power density is given by the relation (24) [43]:

$$\overline{P} = \int_0^\infty P(v) f(v) \mathrm{d}v \tag{24}$$

With $P(v) = \frac{1}{2}\rho s v^3$ representing the power carried by the wind speed v.

By integrating Equation (24), we get the expression of the average available power density given by the relation (25).

$$\overline{P} = \frac{1}{2}\rho c^3 \Gamma\left(\frac{k+3}{k}\right) \tag{25}$$

where ρ represents the density of the air according to the altitude. In this study, we will keep air density constant because its variation is not significant so that it does not impact the calculation of the wind resource [44].

4. Results and Discussions

4.1. Characteristics of the Wind Speed in the Surface Boundary Layer in the Study Area

4.1.1. Vertical Profile of the Wind Speed

The results obtained on the characteristics of wind speed in the surface boundary layer in the study area are summarized as follow. **Figure 2** shows the vertical wind speed profile fitting curves for a typical day, then for the whole month, based on the power law and logarithmic law. **Table 3** summarizes the values of parameters P and H obtained after monthly fitting. The fitting coefficients (α, P, H) obtained is different from one month to another and show that the vertical profile of the wind does not produce the same variations depending on the altitude during the year. The analysis of **Figure 2** shows that the vertical profile of the wind speed fitted by the power law and the logarithmic law corresponds to the measurements whatever the period of the year. RMSE values and MAE coefficients obtained and summarized in **Table 4** are very low and very close. This very low value can be explained by the limited number of measurement level of the wind speed (10 m and 50 m in our study).

Despite this limit, these low values enable us to validate these various fitting equations based on the power law model and the logarithmic law as extrapolation models of the wind speed at the Bobo-Dioulasso site. Both laws can therefore be used to model the profile of the vertical wind speed at our study site as reported by the studies in [23] [45]. Near the ground, there is a significant wind speed variation that would be due to the impact of roughness and obstacles encountered on the ground, which decreases with altitude. **Figure 3** shows the annual best-fit line of the vertical wind profile by applying both laws and the fitting equations. The average annual speed at 10 m above ground using data is 3.02 m/s and 4.39 m/s at 50 m. The estimation errors (RMSE, MAE) between both laws and data measured are very small as abovementioned, *i.e.* 1.40×10^{-15}; 1.33×10^{-15}

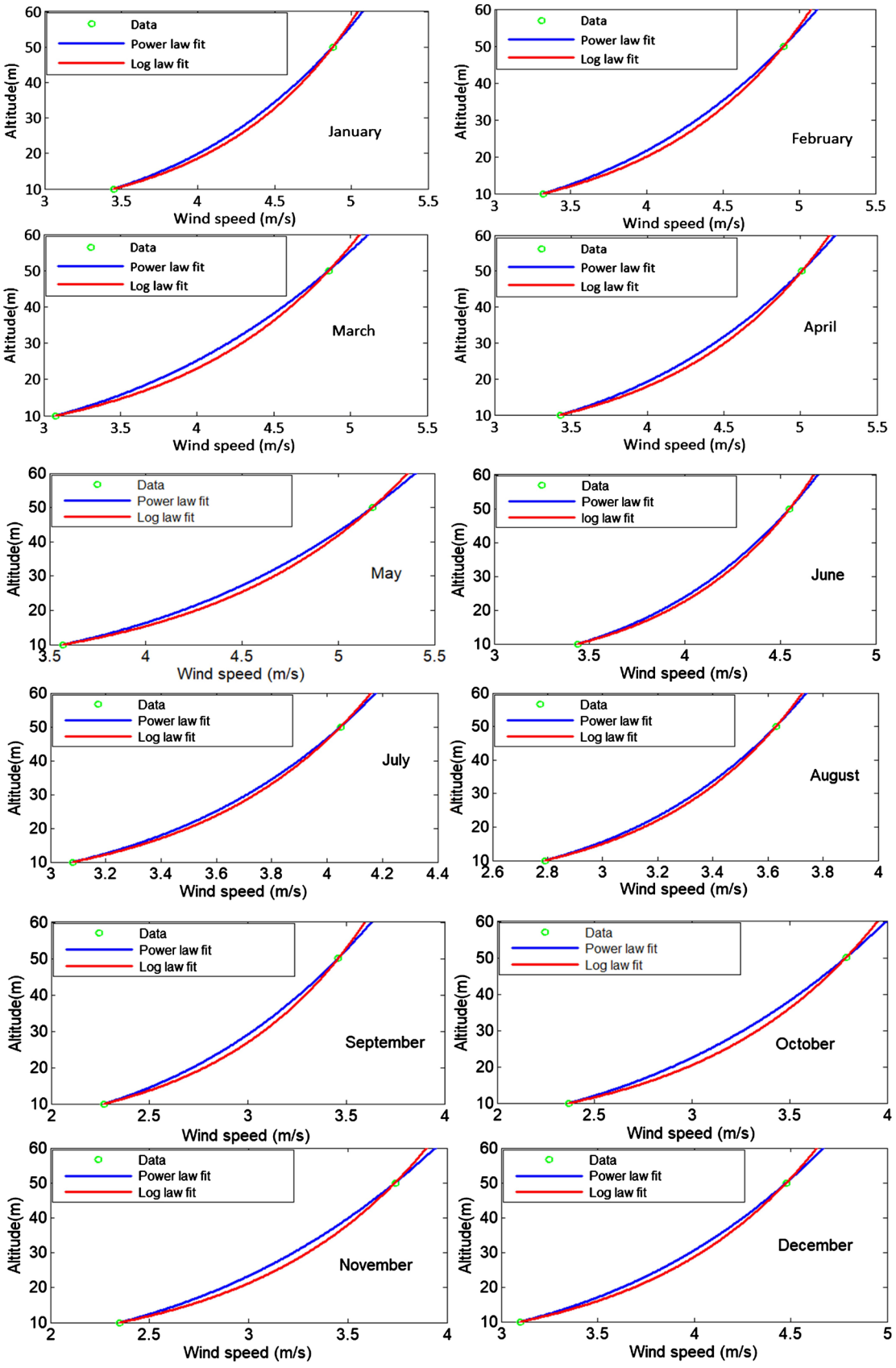

Figure 2. Fitting of monthly wind speed vertical profile from January to December (2006-2016).

Table 3. Parameters to fit log-linear and power law models on Bobo-Dioulasso site.

Month	P	H	α	z_o	u_*
January	0.88	1.40	0.21	0.20	0.35
February	0.98	1.05	0.24	0.33	0.39
March	1.10	0.53	0.28	0.61	0.4
April	0.98	1.169	0.23	0.30	0.39
May	1.00	1.26	0.23	0.28	0.40
June	0.68	1.85	0.17	0.06	0.27
July	0.60	1.69	0.17	0.06	0.24
August	0.52	1.58	0.16	0.04	0.20
September	0.73	0.56	0.26	0.46	0.29
October	0.88	0.33	0.29	0.68	0.35
November	0.86	0.36	0.28	0.65	0.34
December	0.85	1.12	0.22	0.26	0.34
Annual	0.85	1.06	0.23	0.28	0.34

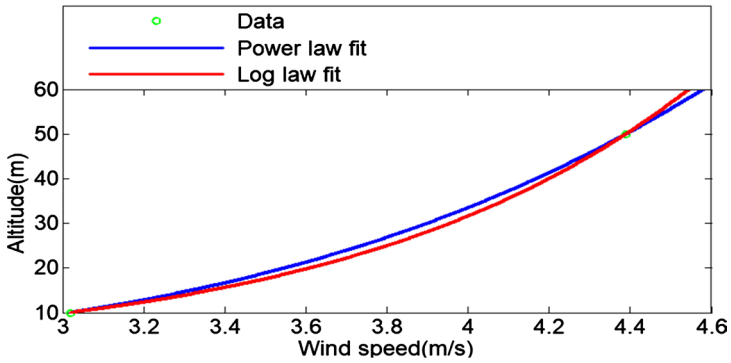

Figure 3. Fitting of the annual wind velocity vertical profile (2006-2016).

and 8.88×10^{-16}; 8.86×10^{-16} respectively for power law and logarithmic law.

4.1.2. Parameters of the Model

Figure 4 shows the average monthly variations of the wind shear parameters. This is the wind shear coefficient (**Figure 4(a)**), the roughness length of the surface (**Figure 4(b)**), and the wind friction speed (**Figure 4(c)**). The coefficients of correlation between the wind shear coefficient and the friction speed, the roughness and the friction speed, as well as the wind shear coefficient and the roughness are estimated at 0.64, 0.55 and 0.90, respectively. These variations show that these three parameters are correlated, notably the shear and the roughness of the soil.

Roughness is an increasing function of wind shear and ground friction speed near the surface. The highest values of these three parameters are observed in March and October, estimated at 0.28; 0.61 m; 0.4 m/s and 0.29; 0.68 m; 0.35 m/s, respectively. In August, the lowest values of the wind shear coefficient, the

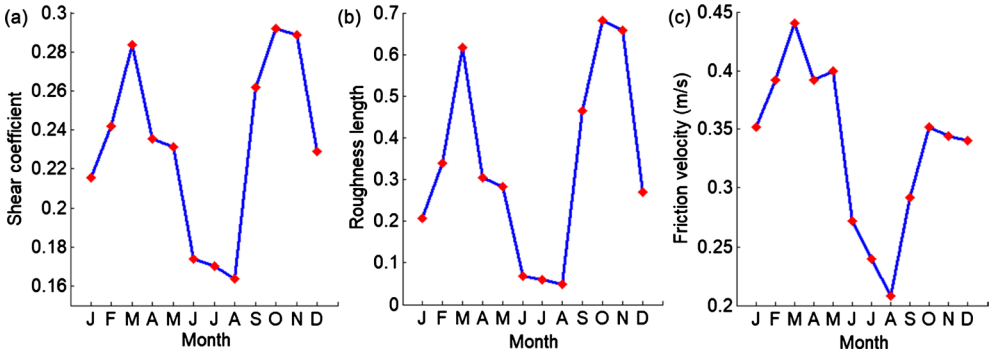

Figure 4. Mean wind shear parameters, (a) mean shear coefficient, (b) mean roughness length, (c)mean shear velocity (2006-2016).

average surface roughness length and the friction speed are estimated at 0.16, 0.04 m and 0.20 m/s, respectively. On an annual basis, the values of the shear coefficient, the average surface roughness length and the friction speed are estimated at 0.23; 0.28 m and 0.34 m/s, respectively. The low values observed for roughness could be due to changes in the soil surface coverage on the site (tree Savannah). The wind direction also influences this variability, notably the various obstacles encountered on the ground (buildings or other structures) and which would be source of cause the high values noticed in March and October. Using the studies in the [46], Hellmann coefficient value indicated for such a zone (tree Savannah) is estimated between 0.24 and 0.33. This result is close to that found on our study site and estimated, on average, between 0.16 and 0.29. When referring to the study by Landry *et al.* [47] on the Burkina Wind Atlas, the roughness length value in this area is between 0.1 m and 1.5 m without taking into account the stability conditions. Our results show that the roughness length values are close to those abovementioned and vary from 0.04 to 0.68 under the same conditions. This gap could be explained by the model (commercial anemoscope Software) and the input data (climate data, topographic data, land use data) used to make estimates in [47].

4.1.3. Comparative Study of Wind Speed Extrapolation Models

Figure 5 and **Figure 6** show a comparison between some wind speed extrapolation models taken in literature, fitting equations requiring fewer parameters and data. It should be noted that the wind shear parameters obtained without taking into account the stability conditions of the atmosphere on our site were used in these extrapolations models. MAE error estimators assessed between measures and models are presented in **Table 5**. The analysis of the results obtained shows that, throughout the year, the fitting equation gives the best fitting of the vertical wind profile with the lowest values of MAE shown in **Table 5**. Considering the annual wind profile, Mikhail model and power 1/7 model underestimate the empirical data while the models by Justus and Mikhail, Kasbadji, and that of the variable coefficient overestimate data, as shown in **Figure 6**. However, in February, April, May, October, November, December, Kasbadji model produces a

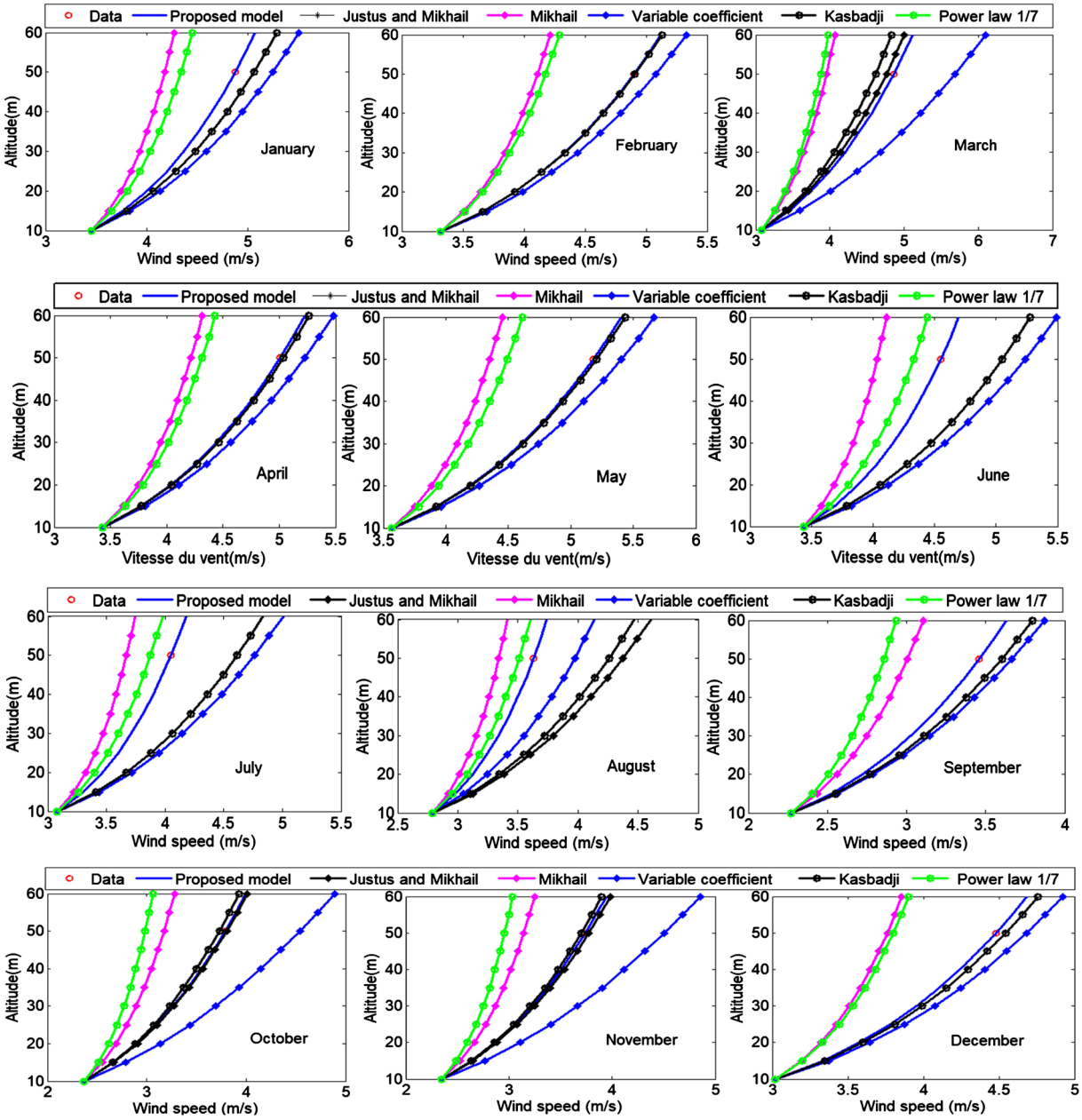

Figure 5. Monthly comparison of wind speed vertical extrapolation models (2006-2016).

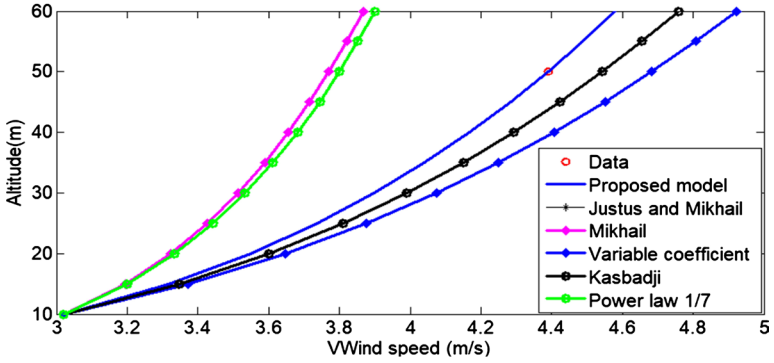

Figure 6. Annual comparison of wind speed vertical extrapolation models (2006-2016).

Table 4. Square root of the mean squared error (RMSE) and the Mean Absolute Error (MAE) for various laws corresponding to the operating range 10 - 50 m (2006-2016).

	Power law		**Logarithmic law**	
	RMSE (10^{-12} m·s^{-1})	**MAE (10^{-12} m·s^{-1})**	**RMSE (10^{-12} m·s^{-1})**	**MAE (10^{-12} m·s^{-1})**
January	0.001	0.001	0.0008	0.0008
February	0.001	0.0006	0.0003	0.0002
March	0.0003	0.0002	0.0006	0.0004
Avpil	0.0003	0.0002	0.001	0.001
May	0.0006	0.0004	0.0006	0.0004
June	0.0008	0.0008	0.0007	0.0006
July	0.0006	0.0004	0.0003	0.0002
August	0.0009	0.0008	0.0008	0.0008
September	0.0008	0.0008	0.0003	0.0002
October	0.001	0.001	0.0003	0.0002
November	0.0009	0.0008	0.0006	0.0004
December	0.001	0.0008	0.0009	0.0006
Annual	0.001	0.001	0.0008	0.0008

Table 5. Mean Absolute Error (MAE) between models and the measure corresponding to the extrapolation range of 10 to 50 m (2006-2016).

	Model proposed	*Justus and Mikhaïl*	*Mikhaïl model*	*Variable coefficient model*	*Kasbadji Model*	*Power 1/7 Model*
	MAE (10^{-12} m·s^{-1})	MAE (m·s^{-1})	MAE (m·s^{-1})	MAE (m·s^{-1})	MAE (m·s^{-1})	MAE m·s^{-1})
January	0.001	0.18	0.35	0.18	0.09	0.26
February	0.0006	0.09	0.39	0.09	0.003	0.36
March	0.0002	0.04	0.45	0.41	0.12	0.49
April	0.0002	0.10	0.39	0.10	0.01	0.34
May	0.0004	0.11	0.41	0.11	0.01	0.34
June	0.0008	0.34	0.25	0.34	0.25	0.11
July	0.0004	0.10	0.39	0.10	0.01	0.34
August	0.0008	0.11	0.41	0.11	0.01	0.34
Sept.	0.0008	0.34	0.25	0.34	0.25	0.11
Oct.	0.001	0.007	0.30	0.37	0.02	0.40
Nov.	0.0008	0.01	0.29	0.38	0.01	0.39
Dec.	0.0008	0.10	0.35	0.10	0.03	0.33
Annual	0.001	0.14	0.30	0.14	0.07	0.29

good fitting with data. The estimation of MAE errors gives 0.003; 0.01; 0.01; 0.02; 0.01; 0.03, respectively. Justus-Mikhail model also provides a good approximation of the wind profile for February, March and November. The estimated MAE values for these months are 0.09; 0.04 and 0.01, respectively. In short, this comparative study also confirms the results of [5] [13] [16] [29] that propose the establishment of an empirical wind extrapolation model for each site.

4.1.4. Vertical Profile of Day and Night Wind Cycle

Figure 7 shows Obukhov length variation during its day and night cycle. Obukhov length is calculated using Equation (5). Referring to Table 2, an analysis of the graphs in this figure shows that from 10 am to 6 pm, the atmosphere is generally unstable while it is stable over the other periods of the day. These results are confirmed by a large number of studies such as those by [23] [46] which show that the atmosphere is unstable during the day.

The lowest values on our study site, recorded in January, February, March,

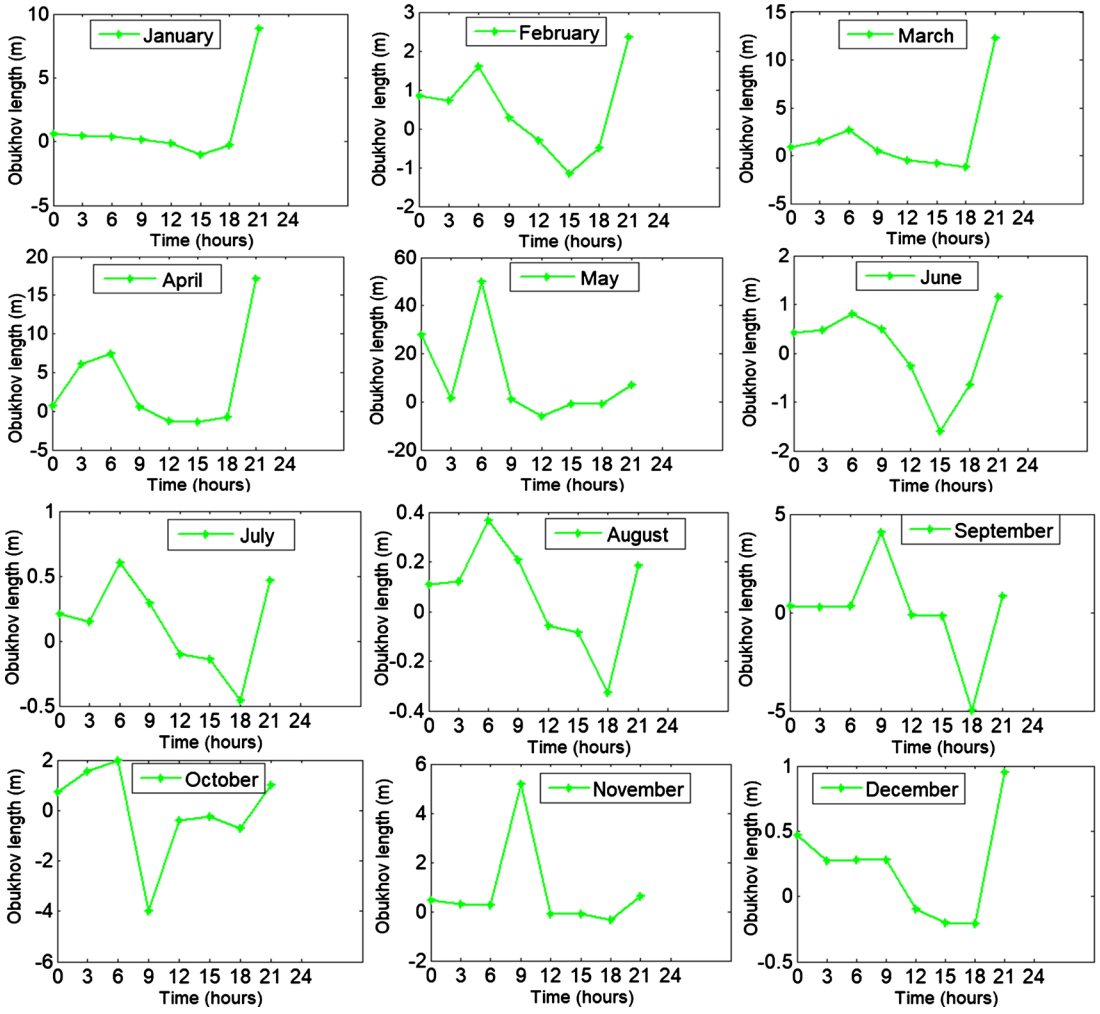

Figure 7. Monthly variation of day and night cycle of Obukhov length for typical day for the Bobo-Dioulasso site (2006-2016).

Table 6. Shear coefficient values according to the atmospheric stability.

Months	J	F	M	A	M	J	J	A	S	O	N	D	Annual
Instable	0.15	0.18	0.24	0.18	0.17	0.10	0.09	0.08	0.21	0.26	0.25	0.16	0.17
Stable	0.21	0.24	0.3	0.24	0.23	0.16	0.15	0.14	0.27	0.32	0.31	0.22	0.23

April, May and June, which correspond to the great part of the dry season in the study area (Bobo Dioulasso), are of −0.47 m, −0.65 m, −0.79 m, −1.16 m, −2.59 m and −0.83 m, respectively. However we record low values in September and October which are −1.75 m and −1.34 m, respectively. The highest values recorded during the unstable period of a typical day in July and August, which correspond to rainy season periods [19], are −0.23 m and −0.15 m, respectively. These results show that during the day and periods of high temperature at the ground level, such as in dry season, the atmosphere is more unstable due to intense convection of air masses. This is consistent with the statements by [6] [29]. In addition, in November and December, months of dry season, values close to those obtained during the rainy season are recorded. They are estimated at −0.19 m, −0.17 m, respectively. These values obtained in November and December could be explained by the gradual arrival of the Harmattan in the study area. Regarding the stable period of the day (from 18:00 to 10:00), highest values are recorded from January to May and vary from 1.5 m (February) to 7.54 m (March) while the months of the rainy season record values that vary between 0.67 m and 1.13 m. Based on these observations, the average vertical wind profile is presented during the daytime cycle between 10:00 and 18:00 and the average profile of the night cycle between 18:00 and 10:00 am. From the power law requiring fewer parameters (Equations (11), (13) and (14)), the wind shear coefficient and wind data recorded at 10 m from the ground, the profiles can be determined by extrapolation following atmospheric stability conditions. **Table 6** summarizes the values of the shear coefficients according to atmospheric stability conditions.

4.2. Variability of Wind Energy Potential on the Study Site

4.2.1. Weibull Distribution Parameters

Table 7 shows the variation of Weibull parameters according to the altitude during the months of the year. We have noticed that both Weilbull parameters (c and k) are an increasing function of the altitude. However, the shape parameter k increases very few according to the altitude, contrary to the scale parameter. The shape parameter k varies from 2.30 in September at 20 m to 2.93 in January at 50 m. The low values of k ($k < 1$) show the predominance of weak winds, $k = 2$ of isotropic conditions, for k values between 1 and 2, winds are scattered in all directions (widespread distribution), while values higher than 2 show the privileged direction (limited distribution) [48]. High k values are encountered during the windiest months while the low ones are during the least windy months. Regarding the scale parameter c, it varies from 3.68 $m \cdot s^{-1}$ in September at 20 m

to 5.58 m·s^{-1} in March at 50 m.

4.2.2. Variation of Wind Energy Density

In Figure 8, the average monthly wind energy density is presented monthly and annually. The wind energy density at the Bobo-Dioulasso site, belonging to the Sudanian climate zone varies according to the months of the year and is strongly influenced by the various seasons of the year (dry season and rainy season). The graph in Figure 8 shows two peaks obtained during the year. The first peak appears on the site in March or May and the second peak in October or December depending on the altitude. The site shows an increase in wind energy from January to May, followed by a decrease from June to August. From September to December, there is an increase again. These various variations were observed between 20 and 30 m altitude. From 40 m to 50 m, the first peak is obtained in March. The period of the year during which wind energy production is at the highest level is therefore from January to June and in December. The unfavorable period of production is from July to November on the study site.

The amount of energy available at 20 m from the ground at the Bobo sites varies from 36.43 W·m^{-2} (August) to 71.13 W·m^{-2} (May). At 50 m from the ground, the power density varies from 45.29 W·m^{-2} (August) to 118.82 W·m^{-2} (March). The average annual power density value is estimated at 53.13 W·m^{-2} at 20 m and at 84.05 W·m^{-2} at 50 m, accounting for 36.78% growth rate.

These various results were compared with studies of [49] [50] carried out on similar sites in West Africa. As a result, in the West African Savanna and Sahelian

Table 7. Shape and scale parameters for the Bobo-Dioulasso site for 20 m, 30 m, 40 m and 50 m.

	Bobo-Dioulasso Site											
	20 m			30 m			40 m			50 m		
	$\overline{v}$	k	c	$\overline{v}$	k	c	$\overline{v}$	k	c	$\overline{v}$	k	c
January	**3.83**	2.90	4.43	**4.07**	2.91	4.70	**4.25**	2.92	4.91	**4.39**	2.93	5.08
February	**3.76**	2.76	4.51	**4.05**	2.77	4.85	**4.26**	2.78	5.11	**4.44**	2.79	5.32
March	**3.64**	2.67	4.48	**4.01**	2.68	4.94	**4.30**	2.69	5.29	**4.54**	2.70	5.58
April	**3.89**	2.68	4.64	**4.19**	2.69	4.99	**4.41**	2.70	5.25	**4.59**	2.71	5.47
May	**4.02**	2.79	4.73	**4.30**	2.80	5.07	**4.52**	2.81	5.32	**4.69**	2.82	5.53
June	**3.69**	2.62	4.42	**3.84**	2.63	4.60	**3.95**	2.64	4.74	**4.04**	2.65	4.84
July	**3.28**	2.45	4.00	**3.40**	2.46	4.15	**3.49**	2.47	4.26	**3.56**	2.48	4.34
August	**2.95**	2.58	3.73	**3.05**	2.59	3.86	**3.12**	2.60	3.95	**3.18**	2.61	4.02
September	**2.62**	**2.30**	3.68	**2.86**	2.31	4.01	**3.04**	2.32	4.26	**3.18**	2.33	4.46
October	**2.84**	2.62	3.77	**3.16**	2.63	4.19	**3.41**	2.64	4.52	**3.61**	2.65	4.79
November	**2.79**	2.66	3.85	**3.09**	2.67	4.26	**3.32**	2.68	4.58	**3.51**	2.69	4.84
December	**3.47**	2.80	4.18	**3.70**	2.81	4.46	**3.88**	2.82	4.67	**4.02**	2.83	4.84
Annual	**3.40**	2.58	4.23	**3.64**	2.59	4.53	**3.82**	2.60	4.76	**3.97**	2.61	4.94

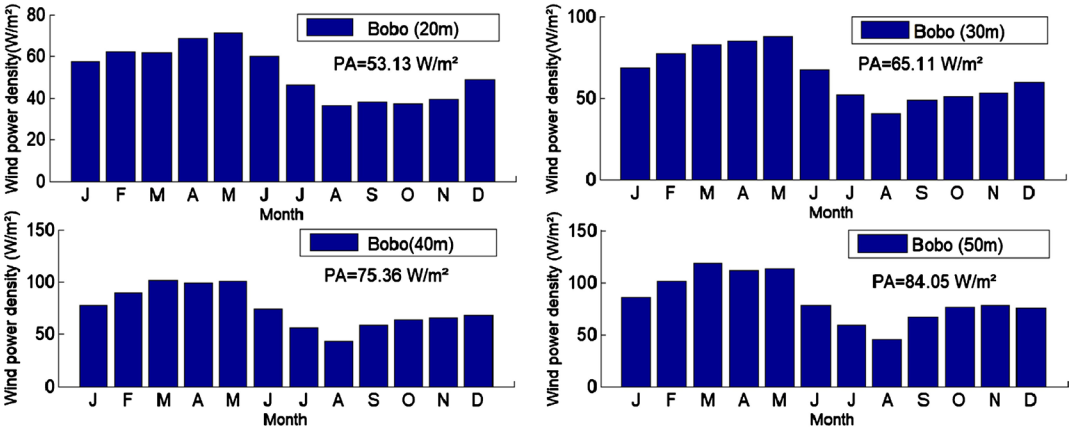

Figure 8. Monthly distribution of the average power density on the Bobo-Dioulasso site from 20 m to 50 m (2006-2016).

zones, particularly in Northern Côte d'Ivoire, Mali, Chad and Niger, wind potential varies from one place to another. This is the case of the Korhogo site in the Savannah zone in Northern Côte d'Ivoire, which wind potential on a monthly basis is more favorable in May, estimated at 29.28 $W{\cdot}m^{-2}$ at 10 m, while on our study sites (Bobo Dioulasso), the maximum value is 49.80 $W{\cdot}m^{-2}$ (May) at the same altitude of 10 m. Our value is therefore higher than that obtained on the site of Korhogo in the North of Côte d'Ivoire. Didane *et al.* [51] conducted a study on the wind potential in Chad and have elaborated a complete wind map of the country. The results show that power density values vary considerably from one area of the country to another. For example, for the Abéché, Am'Timan, Ati, Bokoro, Bousso, Doba, Faya-Largeau, Mao, Mongo, Moundou, N'Djamena, Pala and Sarh sites, the annual wind potentials are 68.80 $W{\cdot}m^{-2}$, 8.04 $W{\cdot}m^{-2}$, 10.06 $W{\cdot}m^{-2}$, 12.21 $W{\cdot}m^{-2}$, 6.73 $W{\cdot}m^{-2}$, 26.03 $W{\cdot}m^{-2}$, 45.29 $W{\cdot}m^{-2}$, 24.07 $W{\cdot}m^{-2}$, 50.54 $W{\cdot}m^{-2}$, 31.41 $W{\cdot}m^{-2}$, 64.63 $W{\cdot}m^{-2}$, 54.80 $W{\cdot}m^{-2}$, 16.58 $W{\cdot}m^{-2}$ at 10 m. As for the Sahelian sites of Goundam, Niafunke, Timbuktu, Koro, Kayes, Gao, Nioro, Bandiagara, Mopti, San, Kangaba, Kadiolo in Mali (day wind potential and night wind potential) at 50 m, the average annual wind potentials are 185 $W{\cdot}m^{-2}$, 170 $W{\cdot}m^{-2}$, 136 $W{\cdot}m^{-2}$, 136 $W{\cdot}m^{-2}$, 122$W{\cdot}m^{-2}$, 119 $W{\cdot}m^{-2}$, 110 $W{\cdot}m^{-2}$, 101 $W{\cdot}m^{-2}$, 95 $W{\cdot}m^{-2}$, 92 $W{\cdot}m^{-2}$, 60 $W{\cdot}m^{-2}$, 51 $W{\cdot}m^{-2}$, respectively. At the Bobo-Dioulasso site (Burkina Faso), the annual wind energy potential is estimated at 84.05 $W{\cdot}m^{-2}$ at 50 m. The differences between our values and those obtained at similar sites could be due to the measurement time scale of the wind data used to perform these various studies or to slightly different climate conditions or the extrapolation models used by some authors. To characterize the sites likely to host wind turbines or large scale wind applications, the [52] studies reported by [53], authors believe that sites can be classified based on their wind power density. Thus, from this table and at 50 m, the areas given in class 1 (0 $W{\cdot}m^{-2}$ to 200 $W{\cdot}m^{-2}$) are generally not suitable for large-scale and economically justifiable wind turbine applications, while class 2 areas (200 $W{\cdot}m^{-2}$ to 300 $W{\cdot}m^{-2}$) are marginal. Areas that can be classified in

Class 3 (300 $W \cdot m^{-2}$ to 400 $W \cdot m^{-2}$) or higher are suitable for most wind turbine applications [52] [53]. Given these and the results presented in **Figure 8**, the study site is not suitable for large scale electrical power generation. But it could be suitable for the installation of small and medium size wind turbines to address electricity deficit in rural areas.

5. Conclusions

This study was conducted in two steps, the first of which consisted of developing specific extrapolation models at the Bobo-Dioulasso site belonging to the Sudanese climate zone in Burkina Faso. The second consists of using these various extrapolation models to assess wind resource at 20 m and 50 m. The power law and the logarithmic law models were therefore assessed for the various classes of atmospheric stability. Parameters of these models were estimated, then these models were compared to the models available in the bibliography. The best model adapted to the site was then used to extrapolate the vertical profile of the day and night cycle from the data measured at 10 m from the ground. The main results of our study on the first phase of our study are summarized as follows:

Power law and logarithmic law give the best fitting of the mean wind speed on a monthly and annual bases. On the site, the atmosphere is generally unstable from 10:00 to 18:00 and stable during the other periods of the day. The mean annual shear coefficients of the wind during the convective day and night cycle are estimated at 0.17 and 0.23, respectively.

The comparative study between wind extrapolation models and data shows that the best fit equation used is always in agreement with data of low MAE values. The development of a model per site is therefore recommended in order to reduce errors in the estimation of wind potential at altitude.

The study of the assessment and the variability of the wind potential between 20 m and 50 m was conducted during months of the year by using the results obtained on the vertical wind profile. The following conclusions can be drawn: Months of the dry season, notably April and May are the windiest of the year.

Wind potential assessed reveals that the largest amounts of energy are generally recorded during months corresponding to the dry season with peaks in March, May or June depending on sites. The amount of energy available in terms of power density at 20 m from the ground at the site varies from 36.43 $W \cdot m^{-2}$ (August) to 71.13 $W \cdot m^{-2}$ (May). At 50 m from the ground, the power density varies from 45.29 $W \cdot m^{-2}$ (August) to 118.82 $W \cdot m^{-2}$. The average annual quantity of power density is estimated at 53.13 $W \cdot m^{-2}$ at 20 m and at 84.05 $W \cdot m^{-2}$ at 50 m, accounting for 36.78% increase rate.

With regard to the power density values, our study site is only suitable for small and medium size wind turbines, producing electrical energy. Specifically, wind turbines with a starting speed ranging between 2 and 3 $m \cdot s^{-1}$ will be valuable. This production can therefore provide people with energy autonomy, particularly in rural areas for activities including pumping water, heating water and

generating electricity. It should be noted that it will be possible to identify a limited number of sites with acceleration effects, located near an existing network, on which a wind farm of medium size and economically feasible can be constructed. These results are therefore useful for those who want to invest in wind energy to efficiently use this source of energy in our country. In the future, the fitting performance of the power and logarithmic laws will be considered for high resolution temporal and multi-level data. This will lead to an optimization of wind energy resource estimate.

Conflicts of Interest

The authors declare no conflicts of interest regarding the publication of this paper.

References

[1] Soulouknga, M.H., Oyedepo, S.O., Doka, S.Y. and Kofane, T.C. (2017) Assessment of Wind Energy Potential in the Sudanese Zone in Chad. *Energy and Power Engineering*, **9**, 386-402. https://doi.org/10.4236/epe.2017.97026

[2] Shawon, M.J., El Chaar, L. and Lamont, L.A. (2013) Overview of Wind Energy and Its Cost in the Middle East. *Sustainable Energy Technologies and Assessments*, **2**, 1-11. https://doi.org/10.1016/j.seta.2013.01.002

[3] Qolipour, M., Mostafaeipour, A. and Rezaei, M. (2018) A Mathematical Model for Simultaneous Optimization of Renewable Electricity Price and Construction of New Wind Power Plants (Case Study: Kermanshah). *International Journal of Energy and Environmental Engineering*, **9**, 71-80. https://doi.org/10.1007/s40095-017-0254-4

[4] Keyhani, A., Ghasemi-Varnamkhasti, M., Khanali, M. and Abbaszadeh, R. (2010) An Assessment of Wind Energy Potential as a Power Generation Source in the Capital of Iran, Tehran. *Energy*, **35**, 188-201. https://doi.org/10.1016/j.energy.2009.09.009

[5] Institut de l'énergie et de l'environnement de la francophonie, numéro 79, deuxième trimestre 2008.

[6] Gualtieri, G. and Secci, S. (2014) Extrapolating Wind Speed Time Series vs. Weibull Distribution to Assess Wind Resource to the Turbine Hub Height: A Case Study on Coastal Location in Southern Italy. *Renewable Energy*, **62**, 164-176. https://doi.org/10.1016/j.renene.2013.07.003

[7] Hau, E. (2013) Wind Turbines: Fundamentals, Technologies, Application, Economics. Springer Science & Business Media, Berlin.

[8] Drechsel, S., Mayr, G.J., Messner, J.W. and Stauffer, R. (2012) Wind Speeds at Heights Crucial for Wind Energy: Measurements and Verification of Forecasts. *Journal of Applied Meteorology and Climatology*, **51**, 1602-1617. https://doi.org/10.1175/JAMC-D-11-0247.1

[9] Monin, A.S. and Obukhov, A.M. (1954) Basic Laws of Turbulent Mixing in the Surface Layer of the Atmosphere. *Contributions of the Geophysical Institute of the Slovak Academy of Sciences*, **24**, 163-187.

[10] Mikhail, A.S. (1985) Height Extrapolation of Wind Data. *Journal of Solar Energy Engineering*, **107**, 10-14.

[11] Justus, C.G. and Mikhail, A. (1976) Height Variation of Wind Speed and Wind Dis-

tributions Statistics. *Geophysical Research Letters*, **3**, 261-264. https://doi.org/10.1029/GL003i005p00261

[12] Gualtieri, G. (2019) A Comprehensive Review on Wind Resource Extrapolation Models Applied in Wind Energy. *Renewable and Sustainable Energy Reviews*, **102**, 215-233. https://doi.org/10.1016/j.rser.2018.12.015

[13] Gualtieri, G. (2016) Atmospheric Stability Varying Wind Shear Coefficients to Improve Wind Resource Extrapolation: A Temporal Analysis. *Renewable Energy*, **87**, 376-390. https://doi.org/10.1016/j.renene.2015.10.034

[14] Gualtieri, G. (2018) Surface Turbulence Intensity as a Predictor of Extrapolated Wind Resource to the Turbine Hub Height: Method's Test at a Mountain Site. *Renewable Energy*, **120**, 457-467. https://doi.org/10.1016/j.renene.2018.01.001

[15] Gualtieri, G. (2017) Wind Resource Extrapolating Tools for Modern Multi-MW Wind Turbines: Comparison of the Deaves and Harris Model vs. the Power Law. *Journal of Wind Engineering and Industrial Aerodynamics*, **170**, 107-117. https://doi.org/10.1016/j.jweia.2017.08.007

[16] Poje, D. and Cividini, B. (1988) Assessment of Wind Energy Potential in Croatia. *Solar Energy*, **41**, 543-554. https://doi.org/10.1016/0038-092X(88)90057-6

[17] Power Data Access Viewer. https://power.larc.nasa.gov/data-access-viewer

[18] Ouedraogo, S., Ajavon, A.S.A., Salami, A.A., Kodjo, M.K. and Bédja, K.-S. (2017) Evaluation of Wind Potential in the Sahelian Area: Case of Three Sites in Burkina Faso. *Research Journal of Engineering Sciences*, **6**, 43-53.

[19] Food & Agriculture Org. (1986) Septieme Reunion du Sous-Comite Ouest and Centre Africain de Correlation des Sols pour la Mise en Valeur des Terres, Ouagadougou, 1985.

[20] Merzouk, N.K., Merzouk, M. and Benyoucef, B. (2007) Extrapolation Vertical des Parametres de Weibull Pour L'Estimation du Potentiel Recuperable. 7.

[21] JITH (2007) Journées internationales de thermique, École des mines d'Albi-Carmaux, Association pour la recherche et le développement des méthodes et processus industriels (France), et Université de Cergy-Pontoise. École des Mines d'Albi-Carmaux, Albi.

[22] Paulson, C.A. (1970) The Mathematical Representation of Wind Speed and Temperature Profiles in the Unstable Atmospheric Surface Layer. *Journal of Applied Meteorology*, **9**, 857-861. https://doi.org/10.1175/1520-0450(1970)009<0857:TMROWS>2.0.CO;2

[23] Donnou, H.E.V. and *al.* (2019) Vertical Profile of Wind Diurnal Cycle in the Surface Boundary Layer over the Coast of Cotonou, Benin, under a Convective Atmosphere. *Advances in Meteorology*, **2019**, Article ID: 7530828. https://doi.org/10.1155/2019/7530828

[24] Bañuelos-Ruedas, F., Angeles-Camacho, C. and Rios-Marcuello, S. (2010) Analysis and Validation of the Methodology Used in the Extrapolation of Wind Speed Data at Different Heights. *Renewable and Sustainable Energy Reviews*, **14**, 2383-2391. https://doi.org/10.1016/j.rser.2010.05.001

[25] Rehman, S. and Al-Abbadi, N.M. (2005) Wind Shear Coefficients and Their Effect on Energy Production. *Energy Conversion and Management*, **46**, 2578-2591. https://doi.org/10.1016/j.enconman.2004.12.005

[26] Spera, A. and Richards, T.R. (1979) Modified Power Law Equations for Vertical Wind Profiles. *Wind Characteristics and Wand Energy Siting Conference*, Oregon, 19-21 June 1979, 1-10.

[27] Gualtieri, G. and Secci, S. (2011) Comparing Methods to Calculate Atmospheric Stability-Dependent Wind Speed Profiles: A Case Study on Coastal Location. *Renewable Energy*, **36**, 2189-2204. https://doi.org/10.1016/j.renene.2011.01.023

[28] Tu, Y.-L., Chang, T.-J., Chen, C.-L. and Chang, Y.-J. (2012) Estimation of Monthly Wind Power Outputs of WECS with Limited Record Period Using Artificial Neural Networks. *Energy Conversion and Management*, **59**, 114–121. https://doi.org/10.1016/j.enconman.2012.02.022

[29] Fritz, B.K., Hoffmann, W.C., Lan, Y., Thomson, S.J. and Huang, Y. (2008) Low-Level Atmospheric Temperature Inversions and Atmospheric Stability: Characteristics and Impacts on Agricultural Applications. *Agricultural Engineering International*, **10**, 1-10.

[30] Nage, G.D. (2016) Analysis of Wind Speed Distribution: Comparative Study of Weibull to Rayleigh Probability Density Function: A Case of Two Sites in Ethiopia. *American Journal of Modern Energy*, **2**, 10-16.

[31] Carta, J.A., Ramírez and Velázquez, S. (2009) A Review of Wind Speed Probability Distributions Used in Wind Energy Analysis. *Renewable and Sustainable Energy Reviews*, **13**, 933-955. https://doi.org/10.1016/j.rser.2008.05.005

[32] Parajuli, A. (2016) A Statistical Analysis of Wind Speed and Power Density Based on Weibull and Rayleigh Models of Jumla, Nepal.

[33] Ouarda, T.B.M.J., Charron, C. and Chebana, F. (2016) Review of Criteria for the Selection of Probability Distributions for Wind Speed Data and Introduction of the Moment and L-Moment Ratio Diagram Methods, with a Case Study. *Energy Conversion and Management*, **124**, 247-265. https://doi.org/10.1016/j.enconman.2016.07.012

[34] Sohoni, V., Gupta, S. and Nema, R. (2016) A Comparative Analysis of Wind Speed Probability Distributions for Wind Power Assessment of Four Sites. *Turkish Journal of Electrical Engineering & Computer Sciences*, **24**, 4724-4735. https://doi.org/10.3906/elk-1412-207

[35] Wais, P. (2017) A Review of Weibull Functions in Wind Sector. *Renewable and Sustainable Energy Reviews*, **70**, 1099-1107. https://doi.org/10.1016/j.rser.2016.12.014

[36] Fagbenle, R.O., Katende, J., Ajayi, O.O. and Okeniyi, J.O. (2011) Assessment of Wind Energy Potential of Two Sites in North-East, Nigeria. *Renewable Energy*, **36**, 1277-1283. https://doi.org/10.1016/j.renene.2010.10.003

[37] Usta, I. (2016) An Innovative Estimation Method Regarding Weibull Parameters for Wind Energy Applications. *Energy*, **106**, 301-314. https://doi.org/10.1016/j.energy.2016.03.068

[38] Kidmo, D.K., Danwe, R., Doka, S.Y. and Djongyang, N. (2015) Statistical Analysis of Wind Speed Distribution Based on Six Weibull Methods for Wind Power Evaluation in Garoua, Cameroon. *Revue des Energies Renouvelables*, **18**, 105-125.

[39] Tizgui, I., El Guezar, F., Bouzahir, H. and Benaid, B. (2017) Comparison of Methods in Estimating Weibull Parameters for Wind Energy Applications. *International Journal of Energy Sector Management*, **11**, 650-663. https://doi.org/10.1108/IJESM-06-2017-0002

[40] Katinas, V., Gecevicius, G. and Marciukaitis, M. (2018) An Investigation of Wind Power Density Distribution at Location with Low and High Wind Speeds Using Statistical Model. *Applied Energy*, **218**, 442-451. https://doi.org/10.1016/j.apenergy.2018.02.163

[41] Usta, I., Arik, I., Yenilmez, I. and Kantar, Y.M. (2018) A New Estimation Approach Based on Moments for Estimating Weibull Parameters in Wind Power Applications. *Energy Conversion and Management*, **164**, 570-578. https://doi.org/10.1016/j.enconman.2018.03.033

[42] Ajayi, O., Fagbenle, R., Katende, J., Ndambuki, J., Omole, D. and Badejo, A. (2014) Wind Energy Study and Energy Cost of Wind Electricity Generation in Nigeria: Past and Recent Results and a Case Study for South West Nigeria. *Energies*, **7**, 8508-8534. https://doi.org/10.3390/en7128508

[43] Rasouli, V., Allahkaram, S. and Tavakoli, M.R. (2015) Application of Adaptability Coefficient in Power Production Evaluation of a Wind Farm. 2015 *Modern Electric Power Systems* (*MEPS*), Wroclaw, 1-6. https://doi.org/10.1109/MEPS.2015.7477167

[44] Ramírez, P. and Carta, J.A. (2005) Influence of the Data Sampling Interval in the Estimation of the Parameters of the Weibull Wind Speed Probability Density Distribution: A Case Study. *Energy Conversion and Management*, **46**, 2419-2438. https://doi.org/10.1016/j.enconman.2004.11.004

[45] Khalfa (2014) Evaluation of the Adequacy of the Wind Speed Extrapolation Laws for Two Different Roughness Meteorological Sites. *American Journal of Applied Sciences*, **11**, 570-583. https://doi.org/10.3844/ajassp.2014.570.583

[46] Peterson, E.W. and Hennessey, J.P. (1978) On the Use of Power Laws for Estimates of Wind Power Potential. *Journal of Applied Meteorology*, **17**, 390-394. https://doi.org/10.1175/1520-0450(1978)017<0390:OTUOPL>2.0.CO;2

[47] Landry, M., Ouedraogo, Y. and Gagnon, Y. (2011) Atlas Éolien Du Burkina Faso.

[48] Pavia, E.G. and O'Brien, J.J. (1986) Weibull Statistics of Wind Speed over the Ocean. *Journal of Climate and Applied Meteorology*, **25**, 1324-1332. https://doi.org/10.1175/1520-0450(1986)025<1324:WSOWSO>2.0.CO;2

[49] Toure, S. and Laoualy, R. (2000) A Theoretical Study of Wind Power Potential in Côte D'Ivoire Using the Weibull Distribution. *Renewables: The Energy for the 21st Century World Renewable Energy Congress VI*, Brighton, 1-7 July 2000, 2304-2307.

[50] Nygaard, I., *et al.* (2017) Feasibility of Wind Power Integration in Weak Grids in Non-Coastal Areas of Sub-Saharan Africa: The Case of Mali. *AIMS Energy*, **5**, 557−584.

[51] Didane, D.H., Rosly, N., Zulkafli, M.F. and Shamsudin, S.S. (2017) Evaluation of Wind Energy Potential as a Power Generation Source in Chad. *International Journal of Rotating Machinery*, **2017**, Article ID: 3121875. https://doi.org/10.1155/2017/3121875

[52] Elliott, D. (1999) Dominican Republic Wind Energy Resource Atlas Development. *SATIS 99 San Juan*, Puerto Rico, 25-27 August 1999, 1-5.

[53] Na, U., A, O. and Ka, I. (2017) Investigation of Wind Power Potential over Some Selected Coastal Cities in Nigeria. *Innovative Energy & Research*, **6**, 156. https://doi.org/10.4172/2576-1463.1000156